MICROCOPY RESOLUTION TEST CHART

NATIONAL BUREAU OF STANDARDS-1963-A

1.0

1.1

1.25

1.4

1.6

1.8

2.0

2.2

2.5

2.8

3.2

3.6

4.0

4.5

5.0

AFGL-TR-85-0184
ENVIRONMENTAL RESEARCH PAPERS, NO. 925

AD-A166 591

Turbulent Heating and Transfer in the Stratosphere and Lower Mesosphere

SAMUEL P. ZIMMERMAN
THOMAS J. KENESHEA

DTIC
SELECTE
APR 1 5 1986
S
D
D

9 August 1985

DTIC FILE COPY

ATMOSPHERIC SCIENCES DIVISION   PROJECT 6670
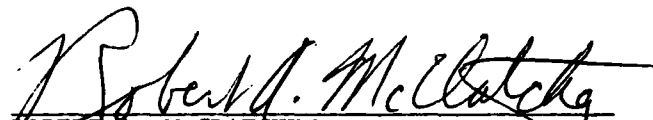# AIR FORCE GEOPHYSICS LABORATORY
HANSCOM AFB, MA 01731

This report has been reviewed by the ESD Public Affairs Office (PA) and is releasable to the National Technical Information Service (NTIS).

"This technical report has been reviewed and is approved for publication"

FOR THE COMMANDER

DONALD D. GRANTHAM
Chief, Tropospheric Structure Branch

ROBERT A. McCLATCHEY
Director, Atmospheric Sciences Division

Qualified requestors may obtain additional copies from the Defense Technical Information Center. All others should apply to the National Technical Information Service.

If your address has changed, or if you wish to be removed from the mailing list, or if the addressee is no longer employed by your organization, please notify AFGL/DAA, Hanscom AFB, MA 01731. This will assist us in maintaining a current mailing list.

Do not return copies of this report unless contractual obligations or notices on a specific document requires that it be returned.

Unclassified

SECURITY CLASSIFICATION OF THIS PAGE

AD-A166591

REPORT DOCUMENTATION PAGE

1a. REPORT SECURITY CLASSIFICATION	1b. RESTRICTIVE MARKINGS
Unclassified	

2a. SECURITY CLASSIFICATION AUTHORITY	3. DISTRIBUTION/AVAILABILITY OF REPORT
	Approved for public release; distribution unlimited.
2b. DECLASSIFICATION/DOWNGRADING SCHEDULE	

4. PERFORMING ORGANIZATION REPORT NUMBER(S)	5. MONITORING ORGANIZATION REPORT NUMBER(S)
AFGL-TR-85-0184 ERP, No. 925	

6a. NAME OF PERFORMING ORGANIZATION	6b. OFFICE SYMBOL (If applicable)	7a. NAME OF MONITORING ORGANIZATION
Air Force Geophysics Laboratory	LYT	

6c. ADDRESS (City, State and ZIP Code)	7b. ADDRESS (City, State and ZIP Code)
Hanscom AFB Massachusetts 01731-5000	

8a. NAME OF FUNDING/SPONSORING ORGANIZATION	8b. OFFICE SYMBOL (If applicable)	9. PROCUREMENT INSTRUMENT IDENTIFICATION NUMBER

8c. ADDRESS (City, State and ZIP Code)	10. SOURCE OF FUNDING NOS.			
	PROGRAM ELEMENT NO.	PROJECT NO.	TASK NO.	WORK UNIT NO.
	62101F	6670	14	05

| 11. TITLE (Include Security Classification) Turbulent Heating and Transfer in the Stratosphere (Contd) | | | | |

12. PERSONAL AUTHOR(S)
Samuel P. Zimmerman, Thomas J. Keneshea

13a. TYPE OF REPORT	13b. TIME COVERED		14. DATE OF REPORT (Yr., Mo., Day)	15. PAGE COUNT
Scientific. Interim.	FROM _____ TO _____		1985 August 9	38

16. SUPPLEMENTARY NOTATION

17.	COSATI CODES		18. SUBJECT TERMS (Continue on reverse if necessary and identify by block number)
FIELD	GROUP	SUB. GR.	Turbulence, Heating momentum,
			Diffusivity, Latitude,
		de	Transfer, $(\text{Aeos} \, \text{W} \, + \, \text{W} - 2.5 \, \text{deg})$

19. ABSTRACT (Continue on reverse if necessary and identify by block number)

The analysis of rocketsonde experimental data from 20 to 70 km altitude and from a latitude band 9.3°N to 76.6°N, grouped around longitude 78°W ± 2.5°, results in the determination of the dynamically and statically unstable regions of the stratosphere and lower mesosphere. Richardson number normalization of the ratio of non-dimensional turbulent to mean parameters, allows us to extrapolate these results to the upper atmosphere. At the Richardson number (R_i) indicated unstable regions, the steady state turbulent energy rate equation is solved, resulting in heat and momentum transfer coefficients, fluxes, and the rate of energy dissipation. Given contiguously unstable regions, the vertical heat and momentum flux divergences are also determined. Summer and winter averages of the results of these analyses are given.

20. DISTRIBUTION/AVAILABILITY OF ABSTRACT	21. ABSTRACT SECURITY CLASSIFICATION
UNCLASSIFIED/UNLIMITED ☐ SAME AS RPT. ☒ DTIC USERS ☐	Unclassified

22a. NAME OF RESPONSIBLE INDIVIDUAL	22b. TELEPHONE NUMBER (Include Area Code)	22c. OFFICE SYMBOL
S. P. Zimmerman	(617) 861-3476	LYT

DD FORM 1473, 83 APR   EDITION OF 1 JAN 73 IS OBSOLETE.   Unclassified

SECURITY CLASSIFICATION OF THIS PAGE

Contents

Accesion For

NTIS CRA&I	☑
DTIC TAB	☐
Unannounced	
Justification	

By

Distribution /

Availability Codes

| Dist | Avail and / or Special |

A-1

iii

QUALITY INSPECTED 3

Illustrations

Turbulent Heating and Transfer in the Stratosphere and Lower Mesosphere

1. INTRODUCTION

The problem of determining turbulence in the upper atmosphere up to the turbo-pause is crucial to the understanding of this region. Not only does turbulence transfer material and heat, but it is also a significant direct source of momentum and heating to and from the mean motions and the thermal mass of the background atmosphere. These heating and transfer rates and the mean height and temporal behavior of turbulence must be ascertained before we will be able to accurately comprehend the spatial and temporal distribution of species, temperature, and motions of all forms (tidal, planetary, and mean) in the mesosphere and lower thermosphere. Until then, models are generated using some known or estimated forcing and damping functions to give a good fit to limited observations.

In this report, we attempt to define some of the major unknowns of atmospheric turbulence that may be important sources and sinks of local heating and transfer of both heat and momentum. Preliminary results leading to this work were reported at the 1979 MAP Symposium.[1] There we demonstrated correspondence between analysis and some required sources and sinks of heat and momentum in the 80 to 90 km region. However, uncertainties in the derivation of the normalized Reynolds

1

stress led us to refine that work. The principle question, we felt, was the validity of assuming that the ratio of the turbulent Reynolds stress to the mean velocity squared, using bounding layer data, is invariant with altitude and only a function of the local stability. We now address the problem of determining an altitude-invariant, normalized and non-dimensional turbulent parameter.
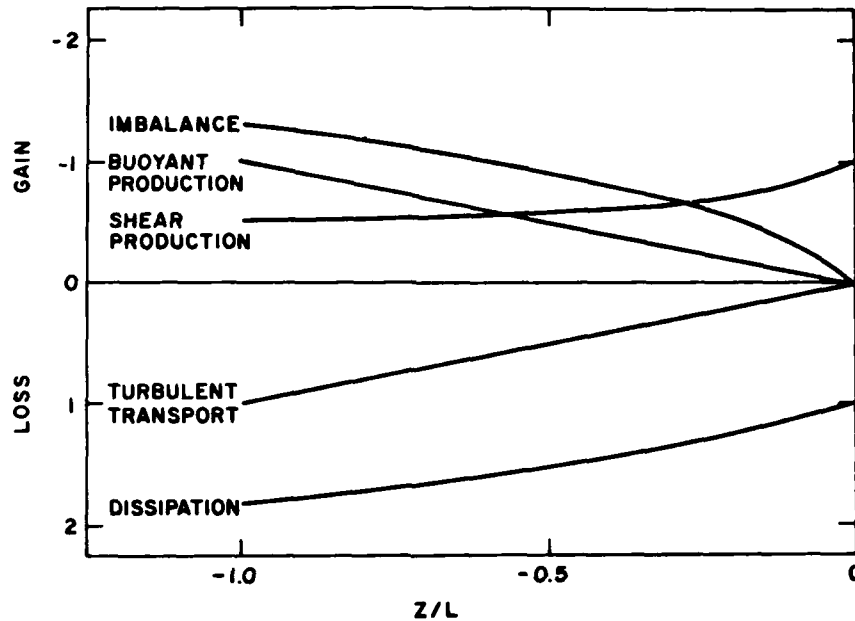
Figure 1. The Schematic Representation of the Dimensionless Energy Budget Under Unstable Conditions (after Figure 7, Wyngard and Cote, 1971[2])

We approach the problem of describing atmospheric turbulence by considering the turbulent energy budget. We shall show that in the boundary layer, for both statically stable and unstable atmospheric regions, the concept of volumetric rate of energy balance of Reynolds stress ($<u' w'> \frac{\partial V}{\partial z}$), heat flow ($\frac{g}{\theta} <w' \theta'>$), and dissipation ($\epsilon$) provides a fairly good description of the local turbulent region, where the sum of Reynolds' stress, heat flux, and dissipation is zero.

2

where

$<u'w'>$ is the turbulent Reynolds' stress,

$<w'\theta'>$ is the turbulent heat flux,

ϵ is the rate of dissipation of turbulent kinetic energy by
kinematic viscosity,

$\frac{\partial U}{\partial z}$ is the local vertical gradient of the horizontal wind (U),

θ is the mean potential temperature $= T \left(\frac{P_o}{P}\right)^{\frac{\gamma-1}{\gamma}}$,

$\frac{\partial \theta}{\partial z}$ is its vertical gradient,

T   is the local kinetic temperature,

g   is the acceleration due to gravity,

P_o is the atmospheric pressure at the earth's surface,

P   is the local pressure,

γ is the ratio of the specific heats (≈ 1.4),

θ' is the fluctuating component of the mean potential temperature,

w'   is the fluctuating vertical velocity, and

u'   is the fluctuating horizontal velocity, and the brackets
denote ensemble averages.

For this study, we have selected what we consider a more logical function for
extrapolation from the boundary layer to the mesosphere than those previously used.[1]
This function is the non-dimensional Reynolds'stres spectral length scale normalized
to the wind length scale. By demonstrating the invariance with altitude of this non-
dimensional ratio, we can apply it to other bodies of wind and temperature data to
determine the turbulent parameters. Using this analysis we present probable values
of the turbulent parameters and their altitude variations from the stratosphere and
into the mesosphere.

2. THEORY

First let us examine the point we raised in the introduction about the assumption
of rate of energy balance between turbulent source and heat loss, or production and
dissipation. Wyngaard and Cote[2] demonstrate that, for boundary layer data and a

---

2. Wyngaard, J.C., and Cote, O.R. (1971) The budget of turbulent kinetic energy
and temperature variance in the atmospheric surface layer, J. Atmos. Sci.,
28:190-201.

positive Richardson number (R_f), this rationale is well established. However, for negative R_f, their values show that generally the balance is nearly maintained with the energy flux terms (Figure 2). This is also shown by Caughey and Wyngaard[3] in a separate work (Figure 3). Thus, the general assumption of energy rate balance that we have made, is fairly well substantiated in lower atmospheric studies.
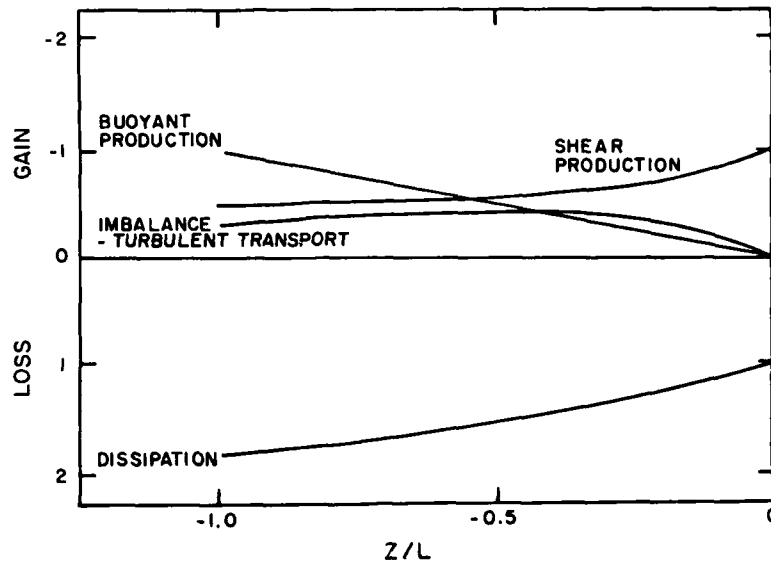
Figure 2. The Same as Figure 1 Except that the Imbalance Has the Turbulence Transport Term Subtracted From it. This suggests that even for negative stability, dissipation is approximately balanced by buoyant production plus shear production

We now consider the spectral relations for the Reynolds stress and heat flux. Following Wyngaard and Cote,[4] and Kaimal et al[5] the Reynolds' stress is expressed as

3. Caughey, S. J., and Wyngaard, J. C. (1979) Some aspects of turbulence structure through the depth of the boundary layer, Quart. J. R. Met. Soc., 105:811-827.

4. Wyngaard, J. C., and Cote, O. R. (1972) Cospectral similarity in the atmospheric surface layer, Quart. J. R. Met. Soc., pp. 590-603.

5. Kaimal, J. C., Wyngaard, J. C., Izumi, Y., and Cote, O. R. (1972) Spectral characteristics of surface layer turbulence, Quart. J. R. Met. Soc., pp. 563-589.

4
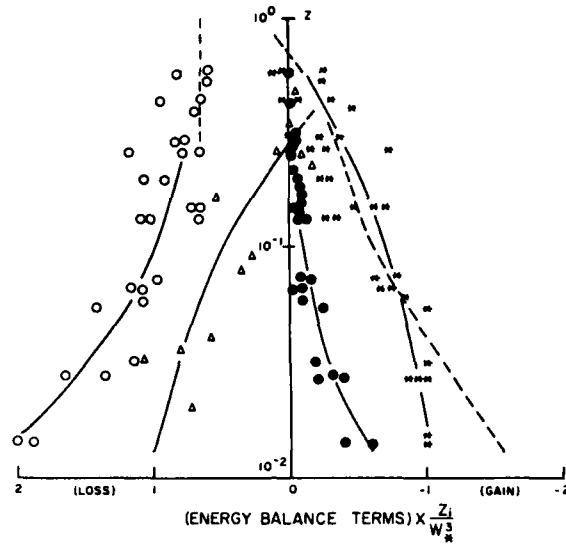
Figure 3. The Same as Figure 2 but for the Data of Caughey and Wyngaard. [3] Components in the energy equation non-dimensionalized with the mixed layer similarity scale $w*$ and z_i, plotted against z/L. The full lines are simply drawn through the data points.

Stars: $\left\{ -\frac{g}{t} <w' T'> \right\} \left\{ Z_i/w_*^3 \right\}$

Solid circles: $\left\{ <u' w'> \frac{\partial V}{\partial Z} + <v' w'> \frac{\partial v}{\partial Z} \right\} \left(\frac{Z_i}{w_*^3} \right)$

Solid triangles: $\left\{ \frac{\partial}{\partial z} (+w' (u'^2 + v'^2 + w'^2)> \right\} \left(\frac{z_i}{w_*^3} \right)$

Open circles: $\epsilon \frac{z_i}{w_*^3}$

Dashed line: Residual

$$<u' w'> = - \zeta_1 \epsilon^{1/3} \frac{\partial V}{\partial z} \int k^{-7/3} dk \qquad (1)$$

and the heat flux as

$$<w' \theta'> = - \gamma_1 \epsilon^{1/3} \frac{\partial \theta}{\partial z} \int k^{-7/3} dk \qquad (2)$$

and where the integration is over the inertial range between wavenumber k_o, the energy containing eddy, and wavenumber k_d, the dissipative scale. ζ_1 and γ_1 are

5

spectral coefficients that are functions not only of Z/L (the ratio of altitude to the Monin-Obunkhoff length scale), but also of the local volumetric Richardson numbers (Kaimal, 1973). The integral is taken only over the inertial spectral function, since shear, dissipation, and temperature gradient are assumed independent of wavenumber.

Now let us consider the simple solution for the heat flux by integrating over the spectrum from k_o (the outer scale of the turbulent spectrum) to ∞. Then Eq. (2) becomes

$$<w'\,\theta'> = -\frac{3}{4}\,\gamma_1\epsilon^{1/3}\frac{\partial\theta}{\partial z}\,k_o^{-4/3}. \tag{3}$$

Solving for $\ell_o (\equiv 1/k_o)$ with the assumption of rate of energy balance and the normalization to the vertical length scale of the mean horizontal wind ($\ell_w = U/\frac{\partial v}{\partial z}$) we arrive at

$$\left(\frac{\ell_o}{\ell_w}\right)^2_{\overline{w'\theta}} = \left(\frac{4}{3\gamma_1}\right)^{3/2}\frac{<w'\,\theta'>}{R_i\,(1-\frac{1}{R_f})^{1/2}\,(\frac{\theta}{g}\frac{\partial\theta}{\partial z})^{1/2}\,\overline{v}^2} \tag{4}$$

Where R_1 is the gradient Richardson number $\left(= \frac{g}{\theta}\frac{\partial\theta}{\partial z}\Big/\left(\frac{\partial\overline{v}}{\partial z}\right)^2\right)$.

Similarly for the Reynolds' stress, we may show

$$\left(\frac{\ell_o}{\ell_w}\right)^2_{\overline{uw}} = \left(\frac{4}{3\zeta_1}\right)^{3/2}\frac{<u'\,w'>}{(1-R_f)^{1/2}\,(\overline{v})^2}. \tag{5}$$

Wyngaard and Cote[4] and Kaimal et al[5] have shown that the heat flux spectral coefficient γ_1 and the stress spectral coefficient ζ_1 are functions of Z/L from 4. to 26 m altitude. However, in the upper atmosphere the Monin-Obukhoff lengths or the boundary layer height cannot be used as scaling factors. Thus we must examine other concepts. Our choice was to find a volumetric scaling factor and then to derive the volumetric relations of γ_1, and ζ_1, as functions of R_f. Then by comparing these determined parameters to the above authors measurements, we can determine the unknown constants.

To solve for these coefficients, we use Eq. (3) and its equivalent for the Reynolds' stress, and substitute the fluctuating buoyancy conditions for the outer scale ℓ_o, where

$$\ell_o \equiv k_o^{-1} = C_1\left[\epsilon/\omega_B^3\right]^{1/2} \tag{6}$$

6

where ω_B is the Brunt-Väissála frequency, $\left(\omega_B^2 = \frac{g}{\theta} \frac{\partial \theta}{\partial z} \right)$.

Again using rate of energy balance to solve for ϵ, γ_1 and ζ_1, it can be shown (Appendix A) that

$$\gamma_1 = -\frac{4}{3 C_1} \left(\frac{R_f}{1 - R_f} \right) , \quad -2.5 < Z/L < -0.3 \tag{7}$$

and

$$\zeta_1 = -\frac{4}{3 C_2} \left(\frac{R_f}{1 - R_f} \right) , \quad -2.5 < Z/L < -0.3 \tag{8}$$

for statically unstable conditions. The constant C_1 is determined by normalization to Figure 2 of Wyngaard and Cote[4] (our Figure 4, open circles). The results (Figure 4) show that for more negative R_f, $C_1 = 1.66$ using Eq. (7) and $C_2 = 1.2$ using Eq. (8).
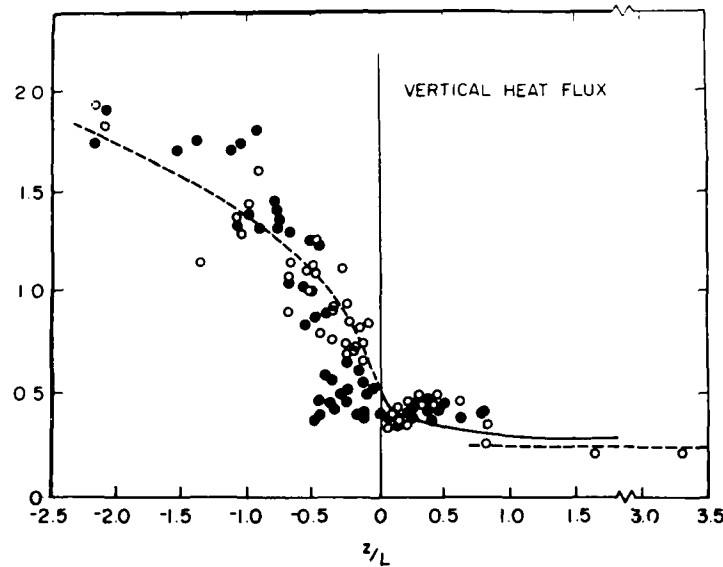
Figure 4. The Vertical Heat Flux Spectral Coefficient α_1 as a Function of Z/L. The open circles are the data of Wyngaard and Cote,[4] and the solid circles from the relations Eqs. (A5) and (A7)

7

For the near neutral and stable region, say $-0.3 < R_f < 0.3$, rate of energy balance has the approximate relation

$$\epsilon \cong <u'w'> \frac{\partial U}{\partial z} ,$$

(9)

and using Eq. (A3) (Appendix A, Eq. (A7)), we observe that

$$\gamma_1 \cong -\frac{4}{3C_1}\left(\frac{R_f}{R_i}\right) .$$

(10)

By normalization to the data $C_3 \equiv 0.65$, and using a similar approach for $<u'w'>$, we see that [Appendix A, Eq. (A10)]

$$\zeta_1 = C_4 \approx 0.35 .$$

(11)

ζ_1 is displayed in Figure 5 for $-2.5 < Z/L < 3$ which is approximately equivalent to $-2.5 < R_f < 0.3$.

Figure 5. The Same as Figure 4 but for the Reynolds' Stress Spectral Coefficient ζ_1

8

As observed there is quite good agreement between γ_1 measured by Wyngaard and Cote[4] and the derived relation Eq. (7) for R_f between these limits. For values of R_f between -0.3 and +0.2 (-0.3 < Z/L, +2.5) the above expression does not fit the observations. However, the empirical relation Eq. (11) describes these res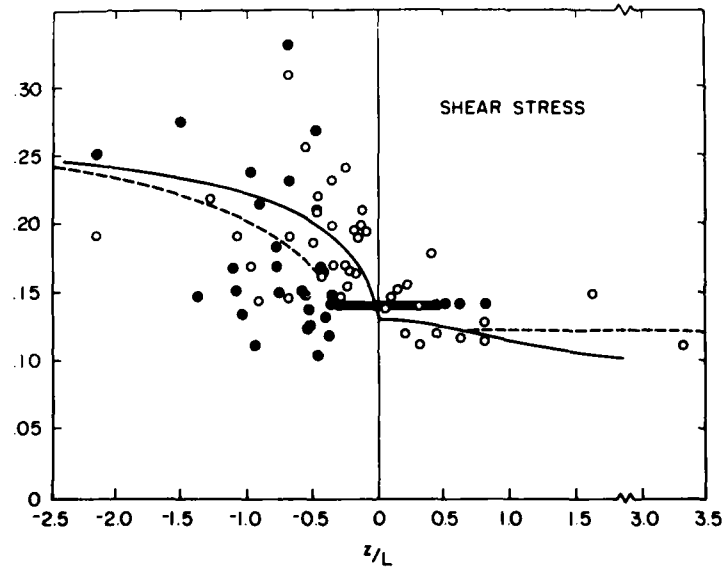ults fairly accurately. The comparison between Eq. (8) and the data points determined from the Kansas experiment[6] are rather scattered, with both analyses showing significant fluctuations around the Kaimal et al empirical curve. Given the relation for γ_1 and ζ_1, we now examine the non-dimensional length scales (4) and (5) using both the Kansas and the Minnesota data bases.[7] Figures 6a and 6b are the representation of Eq. (5) for the Kansas data and the Minnesota data respectively. We see that the large scatter exhibited in the ζ_1 coefficient is not so apparent in this non-dimensional form of the Reynolds' stress for both the unstable, neutral and stable regions. The values displayed in Figure 6b show much greater scatter but they follow quite closely the Kansas results. Figures 7a and 7b show the values from Eq. (4) for the same conditions as described for Figures 6a and 6b. Again we observe quite reasonable results utilizing both bodies of data. Thus, we have demonstrated the existence of a non-dimensional description of the major components of the turbulence rate of energy balance equation from 4 meters to the top of the boundary layer. The observation that the Minnesota results follow quite well and bracket the Kansas results suggests that these non-dimensional scales are a viable way of describing turbulence through the boundary layer. It is definitely not a complete description, since we assume the pressure term and the energy flux term completely balance. But for our purpose, the description of turbulence through the troposphere to the mesosphere, this assumption may be fairly valid. To further ascertain the validity of our results, we examine other data samples obtained by aircraft up to 20 km (Figure 8).[8,9,10] As observed, the non-dimensional heat flux data points fall quite nicely around the calibration curve (the Kansas boundary layer date) to approximately 20 km. Given this normalization, we feel that the extrapolation of these relations to the approximate turbopause (say 100 km) is reasonable.

(Due to the large number references cited above, they will not be listed here. See References, page 25.)
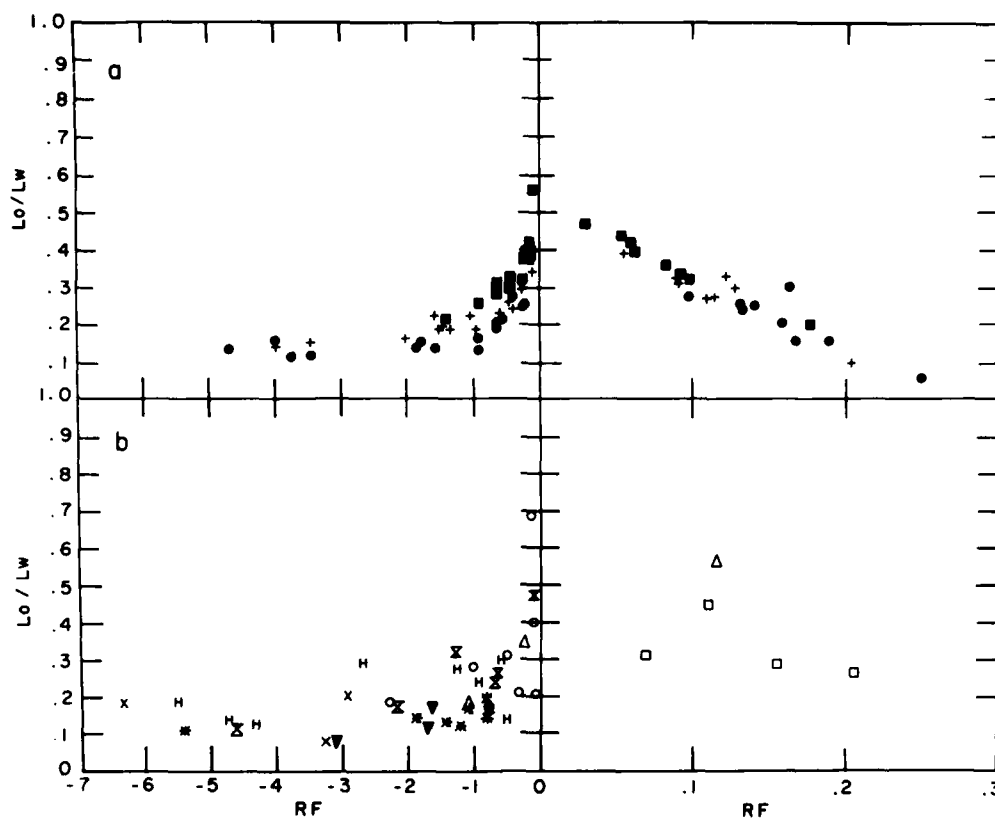
Figure 6. The Representation of the Non-dimensional Reynolds' Stress [Eq. (5)] Using the Boundary Layer Data From: (a) the Kansas Experiment (Izumi[6]) and (b) the Minnesota Experiment (Izumi and Caughey[7]) Respectively. As observed, there is no systematic altitude dependence observed in the analyzed data, and both sets follow quite similarly to each other, for both positive and negative stability. The Kansas results show less variability than that of the Minnesota analysis. We think that this is due to the fine measuring grid used in the Kansas experiment. This would result in better determination of temperature and wind gradients and thus more accurate values of those quantities used in these analyses

Kansas		Minnesota	
■	5. 66 m.	□	12 19 m.
+	11. 31 m.	Δ	9 14 m.
O	22. 63 m.	O	6 10 m.
		H	457 m.
		X̲	305 m.
		X	150 m.
		∇	61 n..
		*	32 m.

10

Figure 7. The Same as Figure 6 Except for the Heat Flux $<w'\theta'>$ [Eq. (4)]

Figure 8. The Same as Figure 7, With the Addition of Measurements From the "High Cat" Data (after Heck and Panofsky[8] and Delay and Dutton[9]) and other results after Kennedy and Shapiro[10]
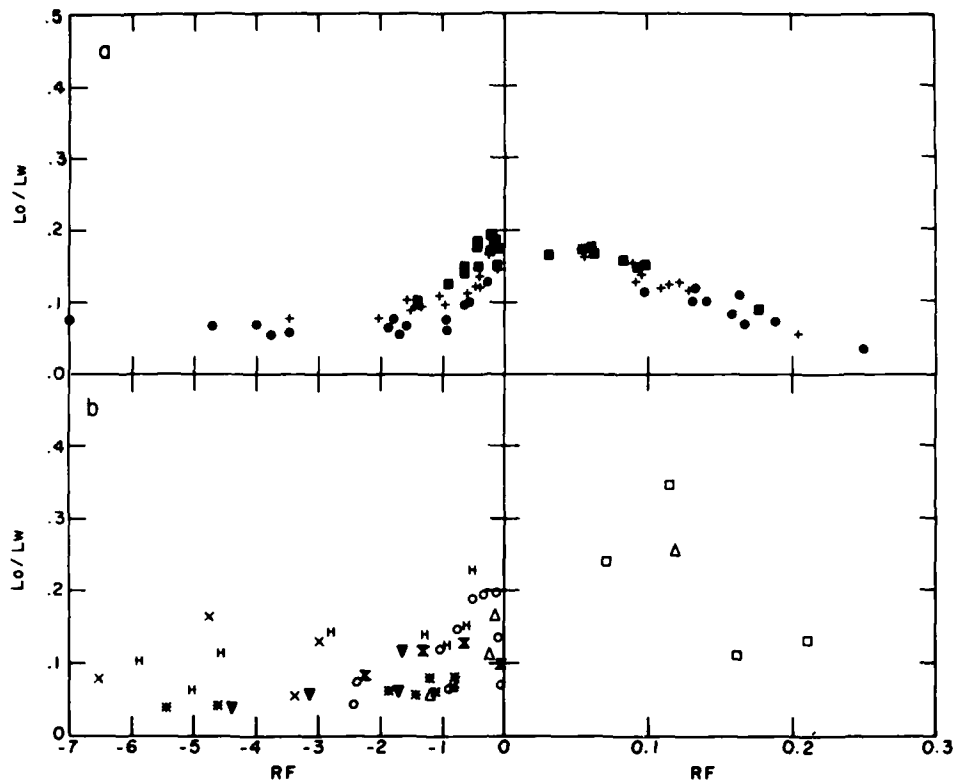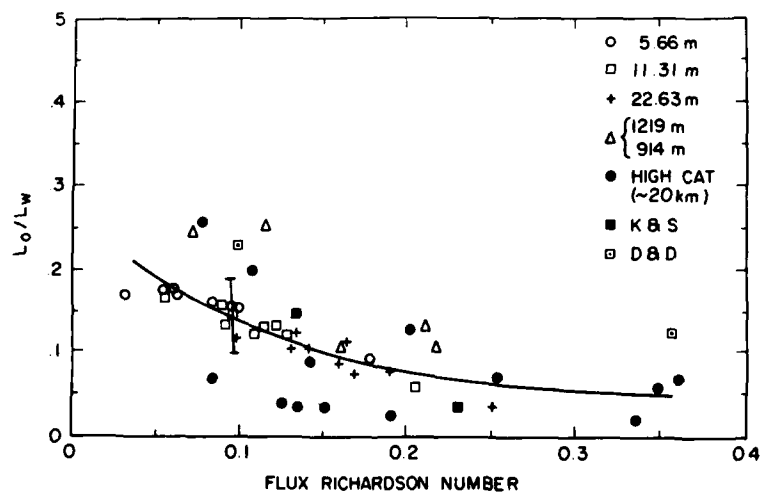
11

3. PREVIOUS ANALYSES AND CONCEPTS

We now analyze for the turbulent transfer coefficients and address here two problem area. First is the question of the critical flux Richardson number (R_{f_c}) and what is its value when the ratio of heat energy transfer by turbulence to direct turbulent heating is unity. This question has been discussed in the literature by many, including work by Hunten,[11] and Izakov.[12] We shall demonstrate here that, contrary to previous works that infer a constant number near unity, this ratio has, within limits, an infinity of numbers.

The second problem area concerns the effects that turbulence has on the mean thermodynamic systems. These are the rate at which turbulence degrades or enhances the mean thermal field, and the production and loss of momentum by turbulence to and from mass motion. In the mesosphere these problems have been addressed by Ebel[13, 14] and by Chandra.[15] Ebel analyzed Groves'[16] model atmospheres for the heating and momentum supply and/or loss that must come from external sources. Chandra[15] following Izakov's[12] analysis, theoretically examined the conditions in the mesosphere and upper stratosphere for local turbulent heating by dissipation and cooling by turbulent transfer, in a steady state energy balance model. He suggests that, for a given flux Richardson number ($R_f = 0.23 = R_{f_c}$), the ratio of cooling by turbulent transfer to heating by dissipation equals unity. For $R_f < 0.23$ the ratio is less than unity and for $R_f > 0.23$ the ratio is greater than unity. Chandra then utilizes a value of $R_f = 0.375$ to calculate the temperature structure, and heat production and loss, of the upper mesosphere and lower thermosphere. We shall examine, in the light of the work presented here, Ebel's and Chandra's results as well as Chandra's assumption. We shall also present determined values of turbulent heat and momentum production, loss and diffusivities.

4. THEORY OF THE MEAN AND TURBULENT HEAT TRANSFER

We will now show how these processes are determined in the atmosphere. Let us start with the heat energy equation, Eq. (12) Chapman and Cowling,[17] Banks and Kockarts,[18] and Izakov.[12]

(Due to the number of references cited above, the will not be listed here.
See References, page 25.)

ENERGY EQUATION

$$\rho\left[\left(C_v \frac{\partial T}{\partial t}\right) + \vec{C}_o \cdot \nabla(C_v T)\right] + P\left(\nabla \cdot \vec{C}_o\right) = -\nabla \cdot \vec{E} + \sum_i Q_i \tag{12}$$

where

$$\vec{E} = -\lambda \nabla T - \overset{\leftrightarrow}{K} \rho C_p \cdot \left(\nabla T + \vec{\Gamma}\right) + T \sum_i C_{p_i} \rho_i \left(\vec{C}_o - \vec{C}_i\right)$$

$\vec{E}$ is the total heat flux vector,

ρ is the mass density,

C_v is the specific heat at constant volume,

C_p is the specific heat at constant pressure,

T is temperature (K)

P is pressure

Q_i are the chemical, turbulent, and radiative heat source and loss,

Γ is the adiabatic lapse rate,

g is the acceleration of gravity,

$\vec{C}_o$ is the mean mass velocity

m_i is the mass of ith species,

C_i is its average velocity, and

$\overset{\leftrightarrow}{K}$ is the turbulent momentum diffusivity tensor.

The turbulent component can be shown (Appendix B) to be equal to the divergence of the vertical heat flux term $<w'\,T'>$ which is the correlation of the vertical velocity and temperature fluctuations,

$$\frac{\partial T}{\partial t} = -\gamma <w'\,T'>\left[\frac{1}{<w'\,T'>}\,\frac{\partial}{\partial t}<w'\,T'> + \frac{1}{\rho}\frac{\partial \rho}{\partial z}\right] \tag{13}$$

where

$<w'\,T'>$ is the turbulent kinetic temperature heat flux,

w' is the vertical component of turbulent velocity, and

T' is the turbulent temperature fluctuation.

Similarly, from the equation of motion

13

$$\frac{\partial \vec{C}_o}{\partial t} = -\frac{1}{\rho}\nabla P + \vec{g} - \frac{1}{\rho}\left\{\nabla \times \left[P \underset{m}{K} + \mu\right] \cdot \left(\nabla \times \vec{C}\right)\right\} . \tag{14}$$

Where we ignore the nonlinear and Coriolis terms, we see that the turbulent vorticity expression reduces to the divergence of the turbulent Reynolds flux,

$$\frac{\partial |\vec{C}_o|}{\partial t} = - <u'w'>\left[\frac{1}{<u'w'>}\frac{\partial}{\partial z}<u'w'> + \frac{1}{\rho}\frac{\partial \rho}{\partial z}\right] . \tag{15}$$

Here the positive and negative values of the turbulent momentum transfer are directed along the wind vector, and

$\vec{C}_o$ is the mean wind vector,

μ/ρ is the kinematic viscosity, and

μ is the molecular viscosity.

Finally, by going to the steady state turbulence energy rate Eq. (16) and using the expression for the flux Richardson number (R_f)

$$- <u'w'>\frac{\partial \vec{U}}{\partial z} \quad \frac{g}{T} <w'T'> = \epsilon \tag{16}$$

we can express the ratio of the heat transfer divergence to turbulent dissipation as (Appendix C)

$$\text{Ratio} = \frac{7}{2}\left(\frac{R_f}{1 - R_f}\right)\left[1 + \frac{H_\rho}{H_{<w'T'>}}\right] \tag{17}$$

where H_ρ and $H_{<w'T'>}$ are the density and heat flux scale heights. Results from this analysis are shown in Figure 9.

We now have relations for determining the local production and loss of heat, momentum and the rate of turbulent dissipation from rate of energy balance. We may determine the diffusivities also, since we have knowledge of the mean tempera- ture and wind fields. These last parameters are simply related by

$$<w'T'> = -K_T\left(\frac{\partial T}{\partial z} + \Gamma\right) \tag{18}$$

and

$$<u'w'> = -K_m\frac{\partial U}{\partial z} \tag{19}$$

14

where K_T and K_m are the turbulent diffusion coefficients of heat and momentum respectively.
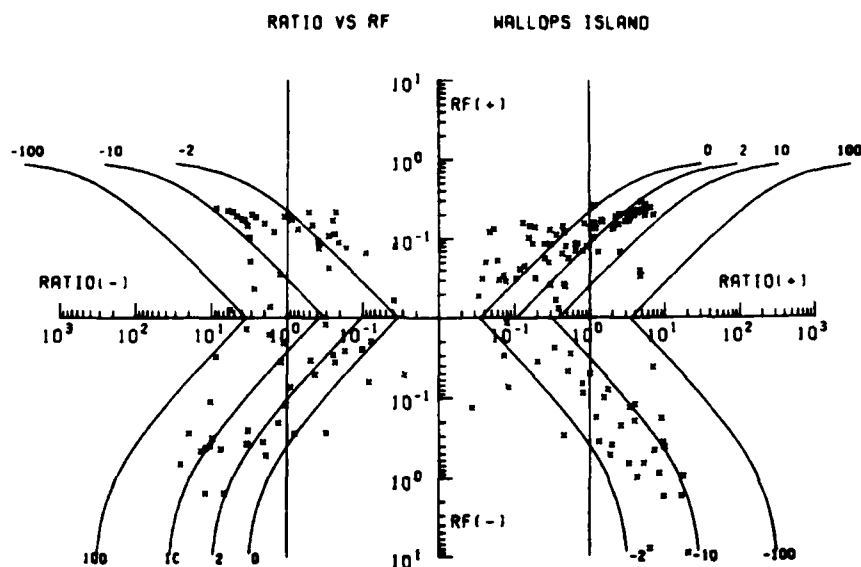
RATIO VS RF   WALLOPS ISLAND

Figure 9. The Ratio of the Turbulent Heat Flux Divergence to the Rate of Turbulent Dissipation (Ratio) as a Function of R_f. Also shown are theoretical curves for different values of $H_0/H <w' \theta'>$ (the ratio of the density scale height to the turbulent heat flux scale heights). The data to the left of the positive vertical line, at the ratio equal to unity, marks the transition area where cooling by turbulent transfer dominates over the heating by dissipation. The remainder of the area denotes effective heating. The right hand side denotes local heating both turbulent transfer and dissipation

5. DATA

The data base used to determine the turbulence coefficients and their winter-summer altitude and latitude variability are the measurements from meteorological rocket network (MRN) covering the period 1969 to 1978. The data consists of wind, temperature and some density measurements, generally at height intervals of 1 km. The data were splined, and the data points were interpolated at 500-m intervals, at which point the derivatives of wind and temperature were determined. Figure 10 is a sample temperature profile showing the measurements, the 500-m spline values and mid-point average values.

15
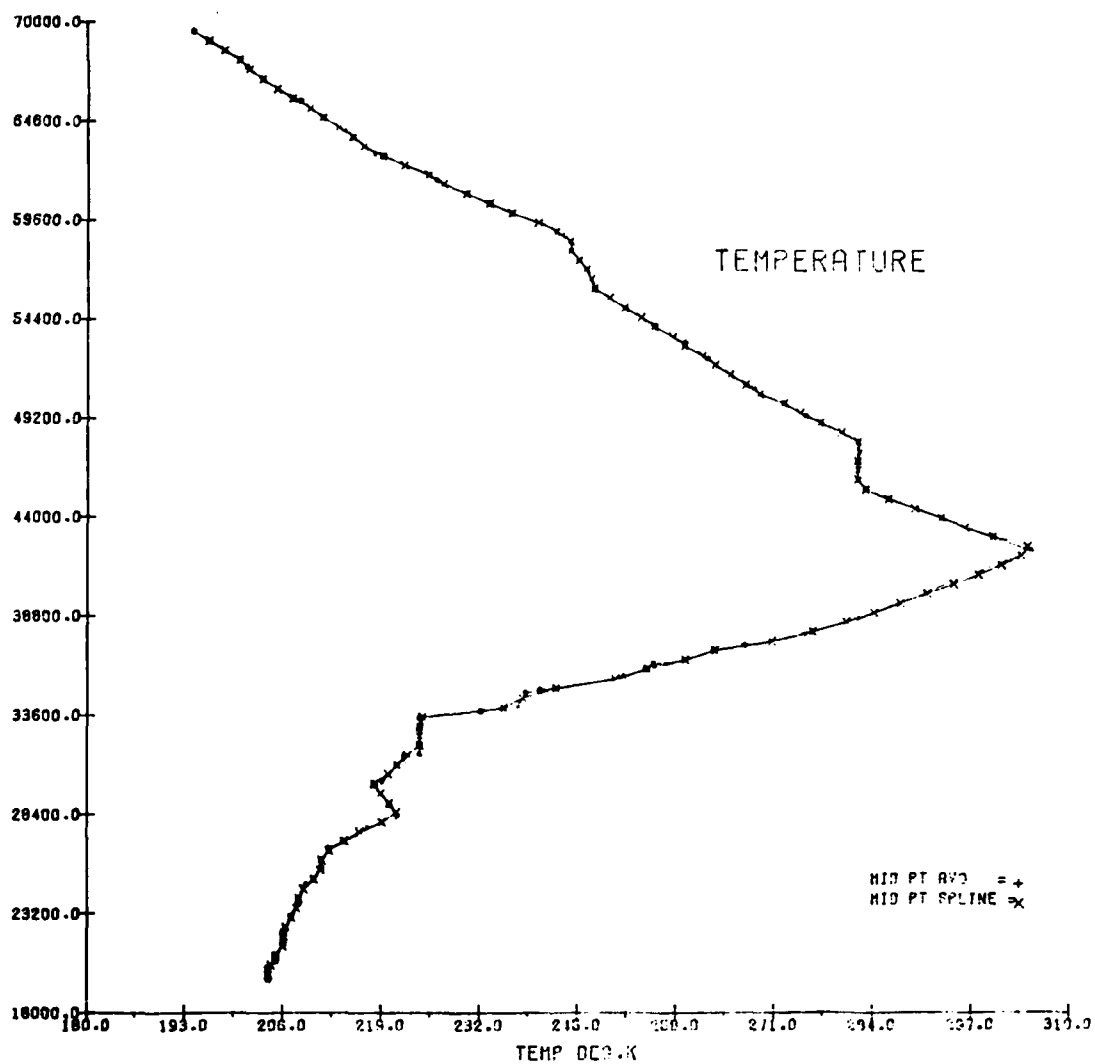
Figure 10. An Example of the Temperature Measurements from 18 to 70 km. The ordinate and abcissa of the measurement are divided into 10 divisions. Superposed on the graphs are the mid-point average (+) and the mid-point spline (x)

These data are from a group of observational sites covering the latitude band, 76. 6° N to 9. 3° N and the narrow longitude band from 75. 5° W to 80. 5° W. In this longitudinal band, extending from the northern most point to as far south as a substantial data base allows, the variability of the turbulence dynamics as a function of northern latitude winter and northern latitude summer is determined.

16

6. RESULTS

Based on the rocket data at Fort Sherman (9.3° N Lat and 80° W Long), Figure 11 shows the statistics of the Richardson number for R_i bin widths of 0.0625. The important feature here is that the most probable R_i's are in the region 0 to 0.187 as contrasted to that of the stratosphere wherein the most probable value is considered to be 0.25.[11] This significant difference reflects strongly the difference between stratospheric and these lower mesospheric microdynamics. This would specify that for a stably stratified turbulent region, the deduced turbulence parameters (K and/or ϵ) determined from the rate of energy balance, would be greatly changed if the value of R_i used was 0.05 rather than 0.25. This has further relevance with regard to the energy balance calculations. Chandra[15] assumed, as a first guess, that the effective value of R_f was ~ 0.375 for the entire stratosphere and mesosphere. This would be a highly stable atmosphere, and, he points out, would insure that in his calculations the divergence of the turbulent heat flux term would always be a positive cooling mechanism over the entire mesosphere. A shift to a lower R_f, say 0.05 in the 70 to 90 km region of the mesosphere would introduce significantly more heating into this region by markedly increasing the turbulent dissipation rate for an adopted diffusivity. However in these data, the other sites show the most probable R_i to be larger than 0.25 and, under these conditions ($R_i \approx 0.25$), Chandra's analysis is more appropriate.

The values of the turbulent parameters determined from these MRS measurements, and within the longitudinal restraints we have imposed, are presented in Figures 12, 13 and 14. The specific locations of these measurements are Thule, Greenland (70.6° N, 68.8° W), Wallops Island, Virginia (37.8° N, 75.5° W), Cape Kennedy, Florida (28.5° N, 80.5° W) and Fort Sherman, Canal Zone (9.3° N and 80° W).

The criteria we used that limited the results to the above sites was that the number of measured observations must be sufficient enough to supply roughly contiguous results within the measured altitude range. This enabled us to compile a meaningful set of measurements to specify the effective values of the turbulent parameters. The parameters analyzed for are the heat diffusivity (K_H), the momentum transfer ($\partial u/\partial t$) and total heating cooling ($\frac{\partial T}{\partial t} + \epsilon$).
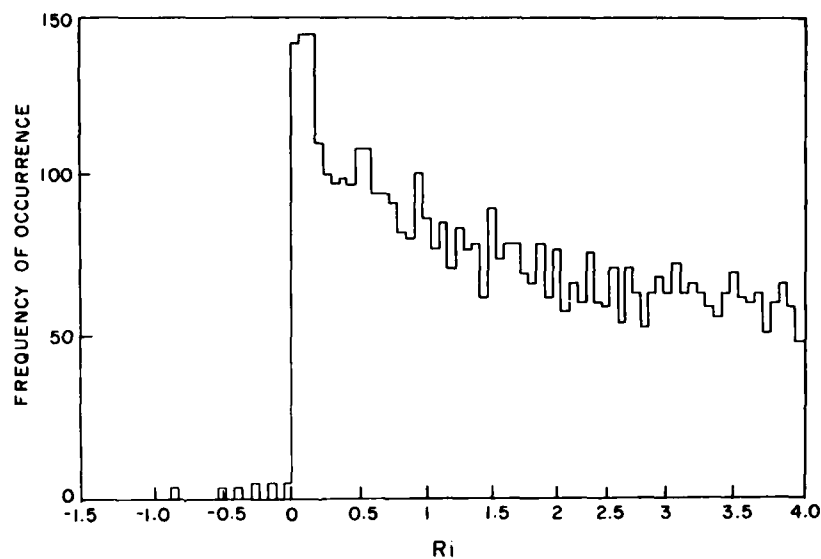
17

Figure 11. Frequency of Occurrences of Richardson Number for Fort Sherman

The values of each of these turbulent parameters, for all sites, are shown in a sequential arrangement along a latitudinal path (Figures 12, 13 and 14) from Thule, Greenland to Fort Sherman, Canal Zone. The winter periods cover the six-month period around the winter solstice. Some of these parameters follow a remarkably sequential profile as a function of altitude considering the nine-year time period of measurement and the logic that we are examining the fluctuating components of wind and temperature. A case in point is the turbulent diffusivity (K_H) measured at the Canal Zone 9.3° N Latitude. As observed (Figure 12) both the winter and summer periods show small variation from a profile that is a function of altitude only. As observed (particularly in Du/Dt) there does not appear to be a balance of energies. This is particularly so because each parameter displayed is over a band of amplitude that would have some effect upon the total dynamics of the atmospheric region. If the amplitude of any parameter fell below the lowest limit of the band, then it would not be displayed in the plot. This is the reason for the extreme paucity of data in the plots of $\partial u/\partial t$ in the northern latitude (Thule) as compared to those of the "Canal Zone".

18
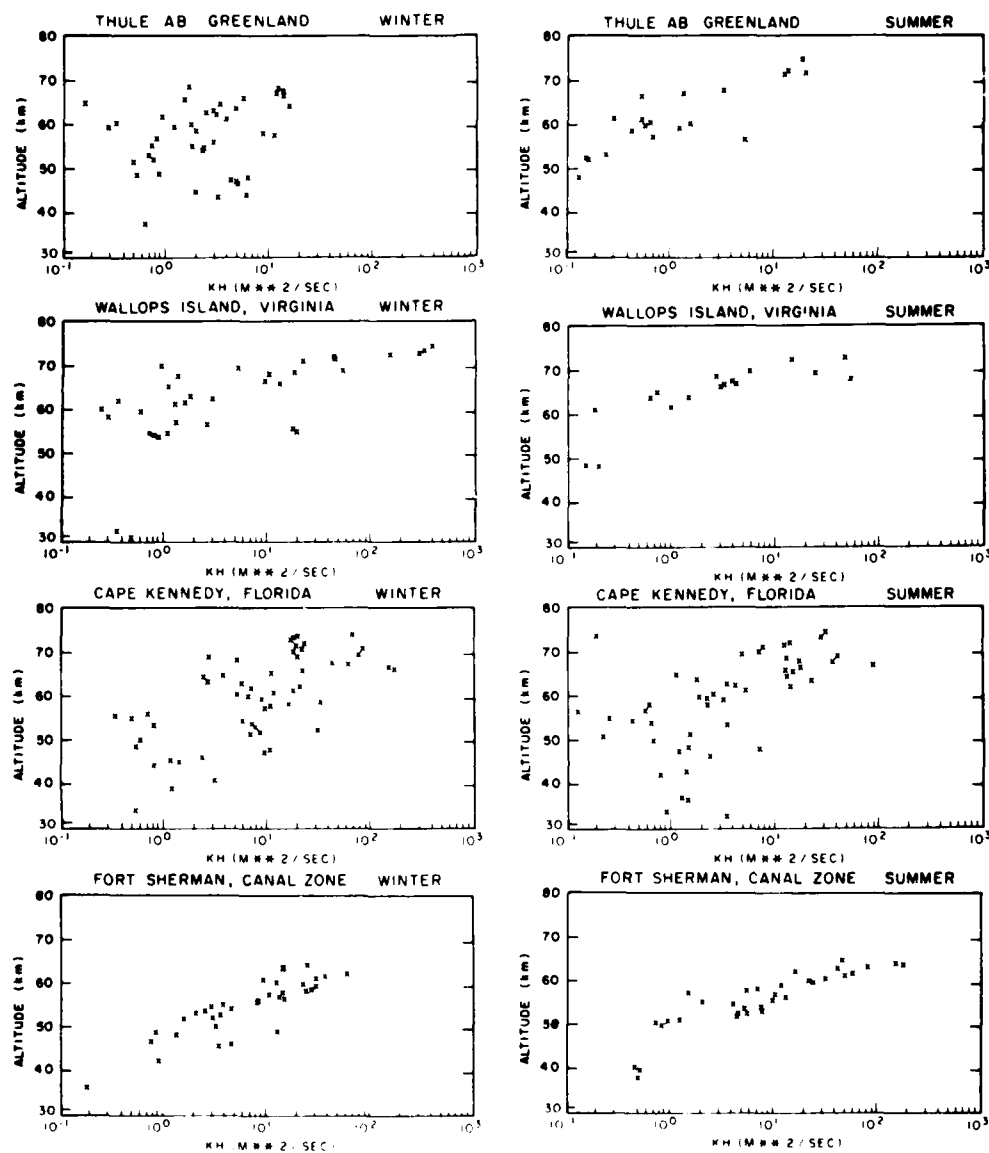
Figure 12. The Latitudinal Distribution of the Turbulent Heat Transfer
Diffusivities (K_H) in units of $m^2 \, sec^{-1}$ for the Four Latitudes 76.6° N,
37.8° N, 28.5° N and 9.3° N. The data has been averaged over a six
months summer and six months winter

Figure 13.   The Same as Figure 10 Except for the Acceleration to and From the Mean Winds in Units of m sec^{-2}

20

Figure 14. The Same as Figure 10 Except for the Net Heat Loss or Gain by Transfer, Both Positive and Negative, and Direct Dissipation (ϵ) in Units of K/sec

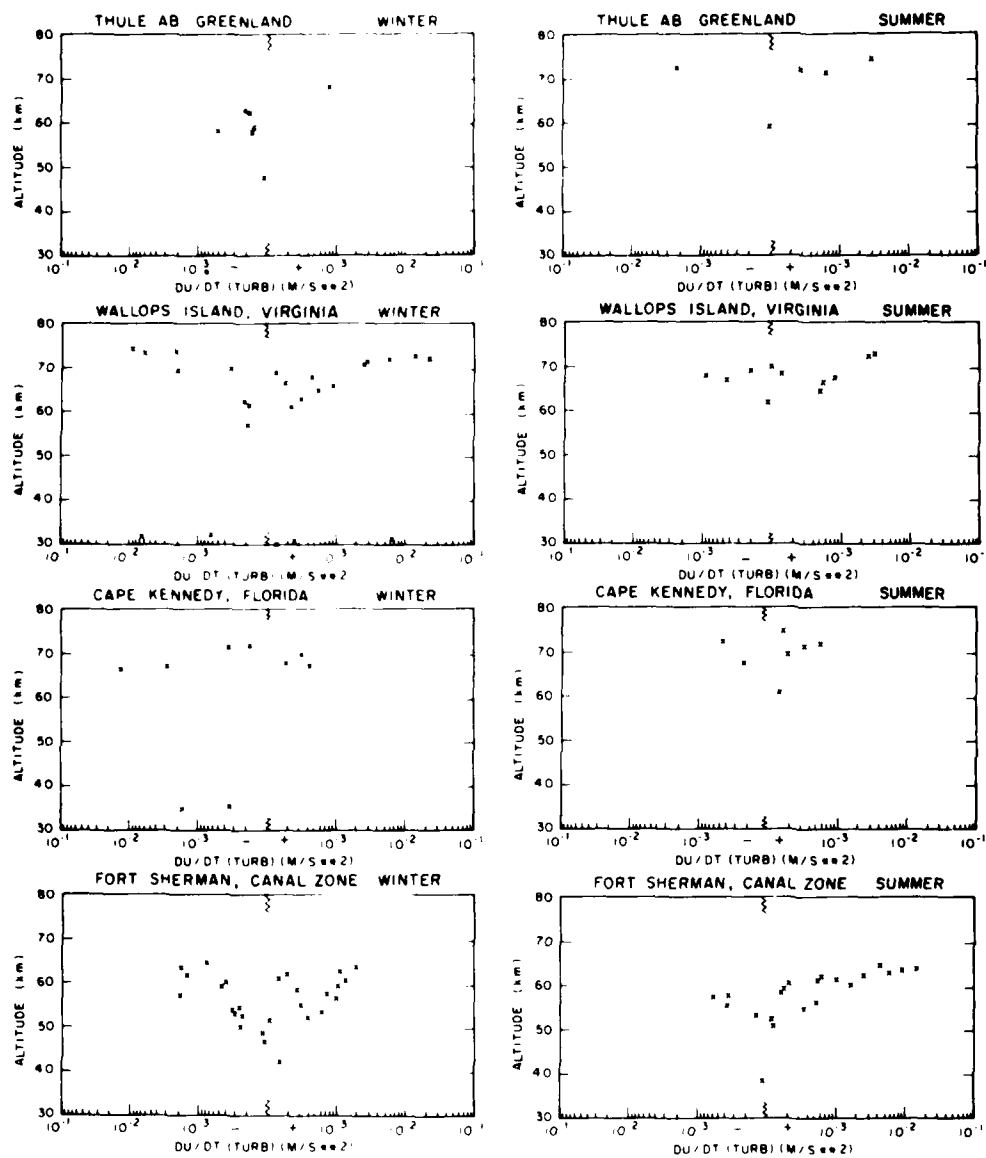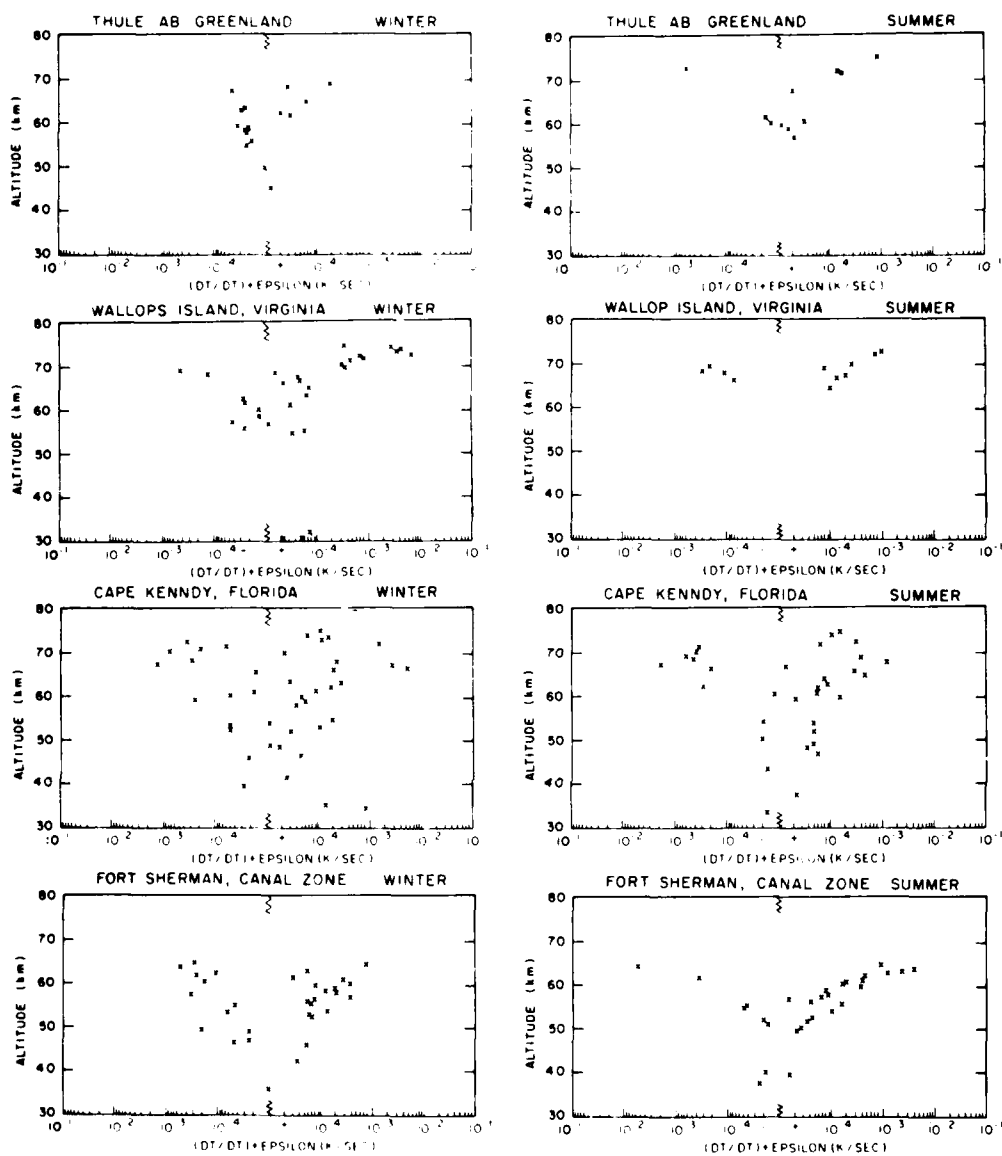Zimmerman and Keneshea,[19] using the same analytic procedure in their examination of the rocket grenade data, noted that the northern latitude (Poker Flat, Latitude 70° N) winters are much more energetic than the summers, and show a higher occurrence rate of turbulence. *Generally, these findings are substantiated* in these analyses, but as observed, this trend is not completely substantiated when we examine other latitudes. The Wallops Island results of K_H *do indeed show this* winter-summer trend as does Cape Kennedy, but the Fort Sherman (Canal Zone) results indicate a reversal of these dynamics, *where the summer turbulence is* more intense than that of the winter.

When considering the diffusivities (K_H) (Figure 12) *we observe the intense* variability of the northern latitude (Thule) winter, and the more uniform behavior of the summer season. *This is similar to the results of the rocket grenade data* (Zimmerman and Keneshea[1, 19]) *but, because of the finer scale of the measurement* grid, we have turbulence measurements to lower altitudes for both winter and summer. This is particularly so for the lower latitudes (Cape Kennedy and the Canal Zone) *where the data shows an almost contiguous profile down to approximately* ~35 km. The Wallops data near 30 km shows a ledge of amplitude diffusivity. This phenomenon was also noted by Zimmerman and Keneshea.[19] These large amplitude energetics are also noted in the turbulent wind acceleration and total heat production and loss mechanisms. Moreover, at Cape Kennedy, we also observe significant winter heating at the lower altitudes, and again, in the summer. There is a *suggestion in these energies that they must be related to a mid-latitude source* constrained in the upper stratosphere, perhaps the "jet stream" that migrates around the mid latitudes. Further analysis of more extensive sites should determine the source of these energies.

The turbulence wind acceleration is generally balanced positive and negative except for the winter at Cape Kennedy, where turulence provides an effective drag *on the wind system,* and at Fort Sherman in the summer, where there is a large net acceleration to the mean winds to the value of 10^{-2} m/sec^2. The total turbulence heating (Figure 14) shows a general balance of heat production and loss in the mid and northern latitudes, but at Cape Kennedy and Fort Sherman for the winter, and around 60 to 70 km, there appears to be a significant loss of heat. In the summer however, at Fort Sherman, turbulence is depositing significant heat into the mesosphere to the value ~ 3×10^{-3} K/sec or ~ 300 K/day.

19. Zimmerman, S. P., and Keneshea, T. J. (1985) Turbulent heating and transfer in the stratosphere and upper mesosphere, J. Atmos. Terr. Phys., to be published.

This initial analysis of the MRN data for turbulence, its amplitudes and sign, substantiates the results of Zimmerman and Keneshea[19] for the Wallops Island data. The results from the other regions along this longitude band show that mesospheric and upper stratospheric turbulence has sufficient energies to significantly modulate mean motions and species distributions.
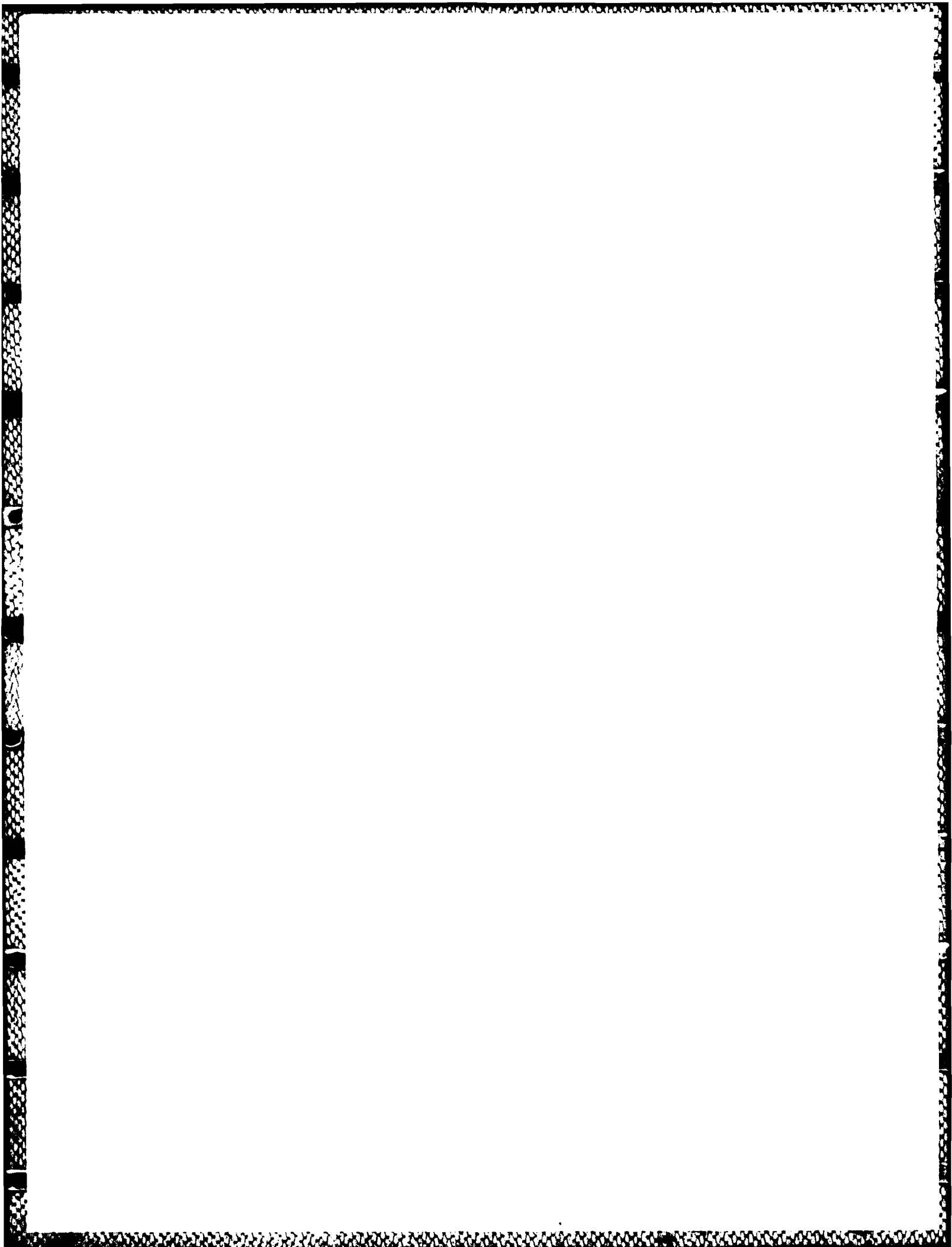
References

1. Zimmerman, S. P., and Keneshea, T. J. (1981) Turbulent heating and transfer in the stratosphere and upper mesosphere, Handbook for MAP, 2:311-322.

2. Wyngaard, J. C., and Cote, O. R. (1971) The budget of turbulent kinetic energy and temperature variance in the atmospheric surface layer, J. Atmos. Sci., 28:190-201.

3. Caughey, S. J., and Wyngaard, J. C. (1979) Some aspects of turbulence structure through the depth of the boundary layer, Quart. J. R. Met. Soc., 105:811-827.

4. Wyngaard, J. C., and Cote, O. R. (1972) Cospectral similarity in the atmospheric surface layer, Quart. J. R. Met. Soc., pp. 590-603.

5. Kaimal, J. C., Wyngaard, J. C., Izumi, Y., and Cote, O. R. (1972) Spectral characteristics of surface layer turbulence, Quart. J. R. Met. Soc., pp. 563-589.

6. Izumi, Y. (1971) Kansas 1968 Field Program Report, ERP, No. 379, AFCRL-72-0041, AD 739165.

7. Izumi, Y., and Caughey, J. A. (1976) Minnesota 1973 Boundary Layer Experiment Data Report, ERP, No. 547, AFCRL-TR-76-0038, AD A023593.

8. Heck, W., and Panofsky, HA. A. (1975) Stratospheric Mixing Estimates From Heat Flux Measurements, the Natural Stratosphere of 1974, CIAP Monograph 1. DOT-TST-75-51, 6-90 to 6-92.

9. Delay, R. D., and Dutton, J. A. (1971) Air analysis of conditions associated with an occurrence of stratospheric CAT, J. Atmos. Sci., 28:1271-1279.

10. Kennedy, P. J., and Shapiro, M. A. (1980) Further encounters with clear air turbulence in research aircraft, J. Atmos. Sci., 37:986-993.

11. Hunten, D. M. (1974) Energetics of thermospheric eddy transport, J. Geophys. Res., 79:2533-2534.

12. Izakov, M. N. (1978) Effect of Turbulence on the Thermal Regime of Planetary Thermospheres, Academy of Sci., USSR, Space Res. Inst., No. 402.

13. Ebel, A. (1974a) Heat and momentum sources of mean circulation at an altitude of 70 to 100 km, Tellus, 26:325-333.

14. Ebel, A. (1980) Eddy diffusion models for the mesosphere and lower thermosphere, J. Atmos. Terr. Phys., 42:617-628.

15. Chandra, S. (1980) Energetics and thermal structure of the middle atmosphere, Planet. Space Sci., 28:585-593.

16. Groves, G. V. (1969) Wind models from 60 to 130 km altitude for different months and latitudes, J. Bri. Interplanet. Soc., 22:285-307.

17. Chapman, S., and Cowling, T.G. (1952) The Mathematical Theory of Non-Uniform Gases, Cambridge University Press.

18. Banks, P.M., and Kockarts, G. (1973) Aeronomy, Academic Press, N.Y.

19. Zimmerman, S.P., and Keneshea, T.J. (1985) Turbulent heating and transfer in the stratosphere and upper mesosphere, J. Atmos. Terr. Phys., to be published.

The calculations in the body of this article are based strongly upon the values of the spectral coefficients γ_1 and ζ_i as functions of the Richardson numbers R_f and R_i. The experimental variation of γ_1 and ζ_1 are demonstrated by Wyngaard and Cote[4] as functions of the ratio of the height of measurement (Z) to the Monin-Obukhoff scale (L). However, for the atmospheric region above the boundary layer, this scaling factor no longer holds and we must utilize the volumetric Richardson numbers in the expressions of these spectral coefficients. Since, as will be shown, no single relation yet explains the measurements for all R_f, we must utilize different derived expressions for these separate, but contiguous, regions of R_f.

To derive these analytic forms of γ_1 and ζ_1, we start with Eq. (3),

$$<w' \theta '> = - \frac{3}{4} \gamma_1 \epsilon^{1/3} \frac{\partial \theta}{\partial Z} k_o^{-4/3} . \tag{A1}$$

Now using the outer scale relation Eq. (6),

$$k_o^{-4/3} = C_1 \left(\frac{\epsilon^{2/3}}{\omega_B^2} \right) . \tag{A2}$$

This is a fluctuating condition, where (ω_B^2) is the square of the Brunt Vaissalla frequency $(= \frac{g}{\theta} \frac{\partial \theta}{\partial Z})$. Equation (A1) then becomes

$$<w' \theta '> = - C_1 \gamma_1 \epsilon \frac{\partial \theta}{\partial Z} \frac{1}{\omega_B^2} . \tag{A3}$$

27

Utilizing rate of energy balance ($<- u'w'> \frac{\partial U}{\partial Z} + \frac{g}{\theta} <w'\theta'> = \epsilon$) to solve for ϵ, and the relation,

$$R_f = \frac{\frac{g}{\theta} <w'\theta'>}{<u'w'> \frac{\partial U}{\partial Z}} , \tag{A4}$$

we solve for γ_1, and arrive at

$$\gamma_1 = \frac{4}{3 C_1} \left(1 - \frac{1}{R_f} \right)^{-1} , \tag{A5}$$

which is Eq. (7) in the main text.

As we observe (Figure 4) this relation normalized to the peak amplitude is only descriptive of the region $-7 < R_f < -0.4$, or $-2.5 < \frac{Z}{L} < \sim -0.3$. For $R_f > -0.4$, there are large deviations from the measured values.

To derive an analytic expression for this region ($-0.4 < R_f < 1$), we again start with Eq. (A1), utilize the outer length scale condition (Kaimel et al[5]), and arrive at

$$k_0^{-4/3} = \frac{C_1 \epsilon^{2/3}}{\left(\frac{\partial U}{\partial Z} \right)^2} , \tag{A6}$$

and observe, using rate of energy balance, that

$$\gamma_1 \longrightarrow \frac{4}{3 C_1} \left(\frac{R_f}{R_i} \right) . \tag{A7}$$

This relation Eq. (A7) does indeed represent γ_1, quite nicely for the region $-0.4 < R_f < 0.2$ [Eq. (A2)].

In a manner similar to the heat flux, we utilize the equation of the spectral Reynolds' Stress,

$$<u'w'> = - \frac{3}{4} \zeta_1 \epsilon^{1/3} \frac{\partial U}{\partial Z} k_0^{-4/3} . \tag{A8}$$

Substituting the fluctuating condition [Eq. (A2)] for k_0, and using rate of energy balance, we arrive at

$$-\zeta_1 = \frac{4}{3 C_2} \left(\frac{R_i}{1 - R_f} \right) \tag{A9}$$

which is Eq. (A8) in the text.

28

Figure 5 shows this [Eq. (A4)] is a fairly good description of ζ_1 for large negative values of R_f, with large deviations as $R_f \to 0$. Using Eq. (A8) and condition Eq. (A6), we observe that

$$\zeta_1 \longrightarrow \frac{4}{3C_2} \tag{A10}$$

for the condition $-0.3 < R_f < 1$. The results (Figure 5) show this relation to be a fair representation of the measurements, which themselves are not in as concise a grouping as those of γ_1.

These analytic functions are used to supply the values of γ_1 and ζ_1 after the local Richardson number has been determined from the wind and temperature data.
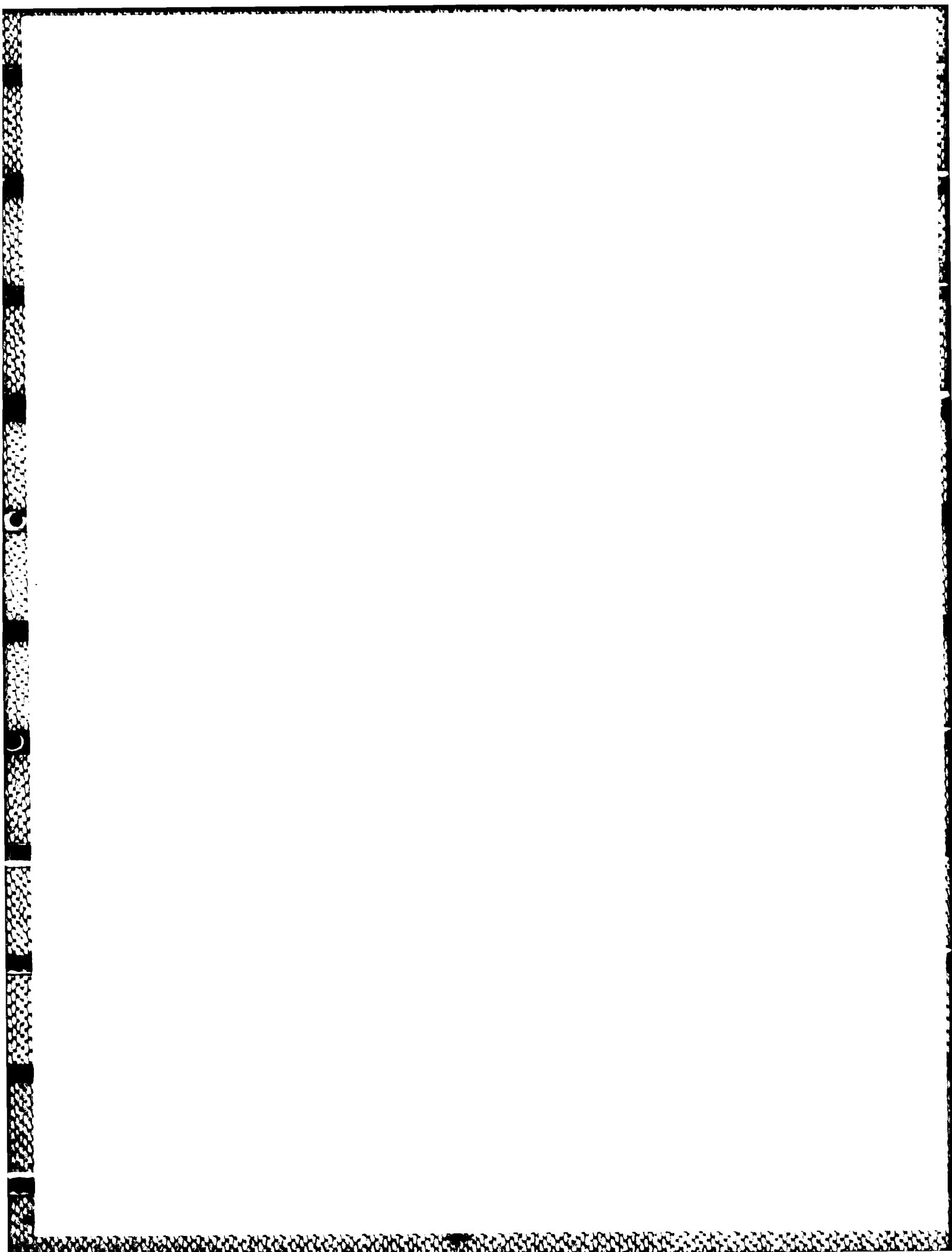
From Eq. (12) we consider only the turbulent terms, and ignore dissipation (ϵ). Thus, in the vertical dimension we have,

$$\frac{\partial T}{\partial t} = \frac{1}{\rho C_v} \frac{\partial}{\partial Z} \left[K_H \rho C_p \left(\frac{\partial T}{\partial Z} + \Gamma \right) \right] . \tag{B1}$$

Setting the ratio of the specific heats equal to γ and using the identity

$$\langle w' T' \rangle \equiv - K_H \left(\frac{\partial T}{\partial Z} + \Gamma \right)$$
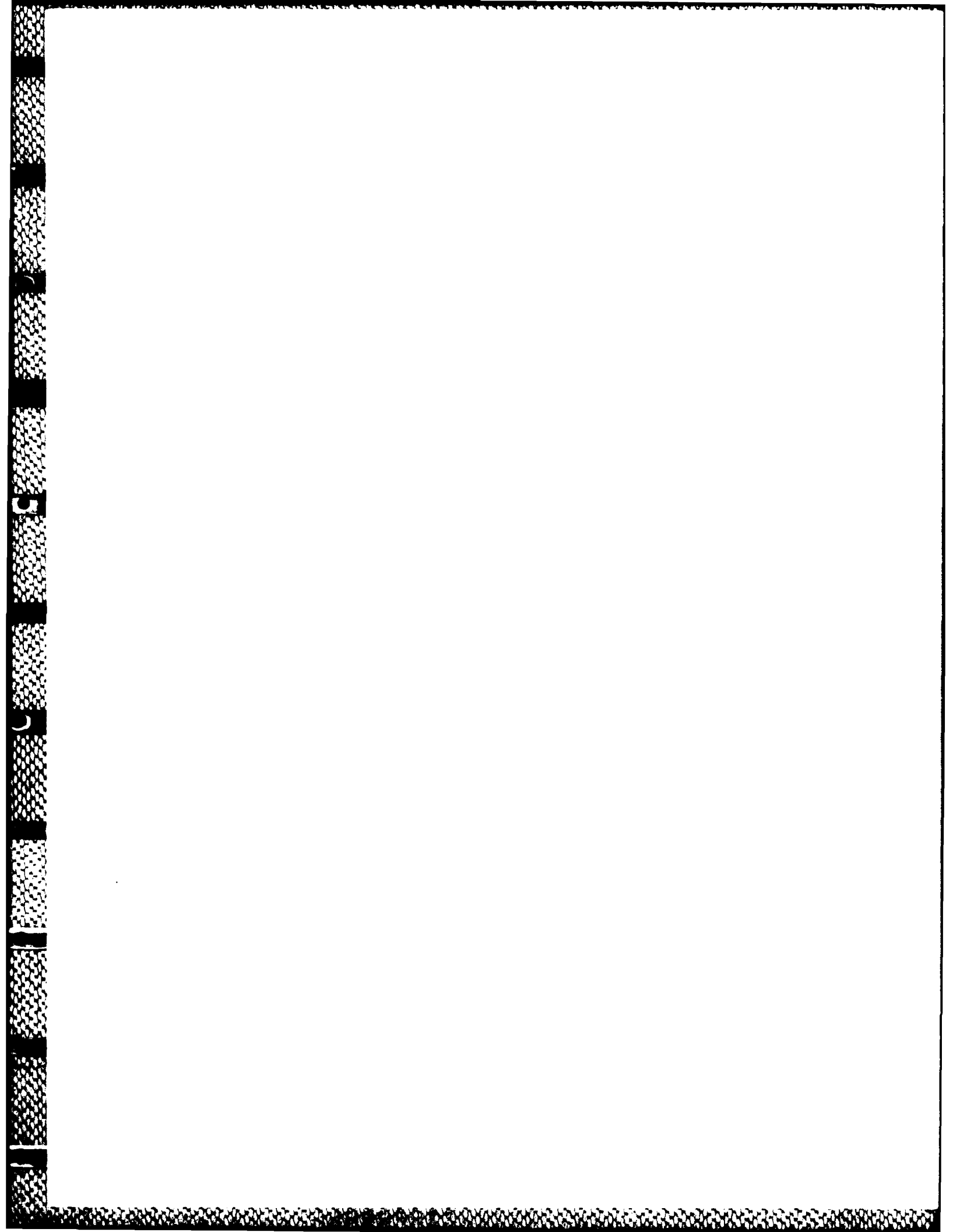
we have

$$\frac{\partial T}{\partial t} = - \gamma \left(\frac{1}{\rho} \frac{\partial}{\partial Z} \right) \left[\rho \langle w' T' \rangle \right] . \tag{B2}$$

Then simply differentiating, we arrive at

$$\frac{\partial T}{\partial t} = - \gamma \langle w' T' \rangle \left[\frac{1}{\langle w' T' \rangle} \frac{\partial}{\partial Z} \langle w' T' \rangle + \frac{1}{\rho} \frac{\partial \rho}{\partial Z} \right] \tag{B3}$$

which is Eq. (13) of the text.

31

The ratio of the divergence of the turbulent heat flux ($< w'\, T'>$) to the rate of turbulent dissipation has been expressed in the text, [Eq. (17)]. We now consider the derivation of this relation.

The ratio (R) is given by,

$$R = \frac{\frac{\partial}{\partial Z}\left[\rho\, C_p < w'\, T'>\right]}{\rho\, \epsilon}, \tag{C1}$$

and by assuming rate of energy balance, $\rho\epsilon$ may be expressed as

$$\rho\epsilon = \left(\frac{1 - R_f}{R_f}\right)\; \frac{\rho g}{T} < w'\, T'>. \tag{C2}$$

Expanding the numerator of Eq. (C1) and rearranging, we have for the ratio

$$R = \frac{C_p\left(\frac{T}{g}\right)}{(1 - R_f)/R_f}\left[\frac{1}{< w'\, T'>}\; \frac{\partial}{\partial Z} < w'\, T'> + \frac{1}{\rho}\; \frac{\partial \rho}{\partial Z}\right]. \tag{C3}$$

Now C_p the specific heat at constant pressure, for a diatomic molecule is equal to $\frac{7}{2}\left(\frac{k}{m}\right)$. Where k is Boltzmann's constant and m is the mass of the molecule. Thus [Eq. (3)] becomes

33

$$R = \frac{7}{2} \left(\frac{R_f}{1 - R_f} \right) \frac{kT}{mg} \left[\frac{1}{H_{\langle w' T' \rangle}} + \frac{1}{H_\rho} \right] \qquad (C4)$$

where $H_{\langle w' T' \rangle}$ is the heat flux scale length, defined as $H_{\langle w' T \rangle} = \dfrac{\langle w' T' \rangle}{\frac{\partial}{\partial Z} \langle w' T' \rangle}$

and H_ρ is the density scale height, defined as $H_\rho = \dfrac{\rho}{(\partial \rho / \partial Z)}$. Since $\dfrac{kt}{mg}$ is the atmospheric pressure scale length Hp, we then have

$$R = \frac{7}{2} \left(\frac{R_f}{1 - R_f} \right) \left[\frac{H_p}{H_{\langle w' T' \rangle}} + \frac{H_p}{H_\rho} \right] . \qquad (C5)$$

We now assume that Hp $\approx$ H_ρ, which specifies that Ht (the temperature scale length) $\gg$ H_ρ. According to the U.S. Standard Atmosphere (1976) this is a fairly valid assumption, throughout the atmosphere. The ratio then becomes

$$R \cong \frac{7}{2} \left(\frac{R_f}{1 - R_f} \right) \left[1 + \frac{H_\rho}{H_{\langle w' T' \rangle}} \right] . \qquad (C6)$$

This relation [Eq. (C6)], for values of $(H_\rho / H_{\langle w' T' \rangle})$ equal to -100, -10, -2, 0, 2, 10, and 100, are included in Figure 9 as the solid curved lines.

END

DTIC

5-86